Available online at www.sciencedirect.com
SCIENCE DIRECT
Journal of Colloid and Interface Science 283 (2005) 160–170
JOURNAL OF Colloid and Interface Science
www.elsevier.com/locate/jcis

Sorption of the antibiotic ofloxacin to mesoporous and nonporous alumina and silica

Keith W. Goyne [a], Jon Chorover [a,*], James D. Kubicki [b], Andrew R. Zimmerman [c], Susan L. Brantley [b]

[a] *Department of Soil, Water and Environmental Science, University of Arizona, 429 Shantz Building, Tucson, AZ 85721-0038, USA*
[b] *Department of Geosciences, The Pennsylvania State University, University Park, PA 16802, USA*
[c] *Department of Geological Science, University of Florida, Gainesville, FL 32611, USA*

Received 23 June 2004; accepted 17 August 2004

Available online 30 November 2004

Abstract

Mesoporous and nonporous SiO_2 and Al_2O_3 adsorbents were reacted with the fluoroquinolone carboxylic acid ofloxacin over a range of pH values (2–10) and initial concentrations (0.03–8 mM) to investigate the effects of adsorbent type and intraparticle mesopores on adsorption/desorption. Maximum ofloxacin adsorption to SiO_2 surfaces occurs slightly below the pK_{a2} (pH 8.28) of the antibiotic and sorption diminishes rapidly at pH > pK_{a2}. For Al_2O_3, maximum sorption is observed at pH values slightly higher than the adsorbent's point of zero net charge (p.z.n.c.) and less than midway between the pK_a values of ofloxacin. The effects of pH on adsorption and ATR–FTIR spectra suggest that the zwitterionic compound adsorbs to SiO_2 solids through the protonated N_4 in the piperazinyl group and, possibly, a cation bridge; whereas the antibiotic sorbs to Al_2O_3 solids through the ketone and carboxylate functional groups via a ligand exchange mechanism. Sorption edge and isotherm experiments show that ofloxacin exhibits a higher affinity for mesoporous SiO_2 and nonporous Al_2O_3, relative to their counterparts. It is hypothesized that decreased ofloxacin sorption to mesoporous Al_2O_3 occurs due to electrostatic repulsion within pore confines. In contrast, it appears that the environment within SiO_2 mesopores promotes sorption by inducing formation of ofloxacin–Ca complexes, thus increasing electrostatic attraction to SiO_2 surfaces.

Keywords: Ofloxacin; Fluoroquinolone carboxylic acid; Mesoporosity; Sorption edge; Adsorption/desorption isotherms; ATR–FTIR spectroscopy; Molecular modeling; Mineral–organic interactions

1. Introduction

Fluoroquinolone carboxylic acids (FQCAs) are a class of chemotherapeutic agents with antibacterial activity used in human and veterinary medicines. Although absorptivity of orally administered FQCAs is high [1], a portion of the dose passes through the body into human and animal excrement. Thus, FQCAs have been detected in wastewaters insufficiently treated by sewage treatment plants [2,3], liquid animal manures [4], and streams [5]. Recent studies in the United States and Europe have documented the presence of FQCAs in wastewaters and streams with concentrations typically reported in the range of ng L^{-1} to μg L^{-1} [2,5–7]. Due to the land application or discharge of wastes to streams and our limited knowledge of the fate and interactions of FQCAs in aquatic and terrestrial environments, these compounds are of significant environmental concern [3,5,8].

Within the large class of FQCAs, ofloxacin is used to treat urinary and respiratory tract infections in humans and animals [9]. Although a significant number of studies have investigated aqueous ofloxacin–metal complexation reactions [9–14], much less work has been done on the sorption of ofloxacin to minerals and soil. Djurdjevic et al. [13] determined that sorption of ofloxacin to Al_2O_3 solids exhibited S-shaped isotherms when experiments were conducted

* Corresponding author. Fax: +1(520)-621-1647.
E-mail address: chorover@cals.arizona.edu (J. Chorover).

0021-9797/$ – see front matter
doi:10.1016/j.jcis.2004.08.150

from 19 to 140 μmol L^{-1} in neutral and very acidic (pH 1) aqueous background solutions, and isotherms were L-shaped (Langmuir) in basic solutions (pH 11). The greatest extent of sorption occurred at neutral pH (0.7 mmol g^{-1}) followed by sorption at pH 1 (0.5 mmol g^{-1}) and sorption at pH 11 (0.38 mmol g^{-1}) [13]. However, ofloxacin sorption onto $Al(OH)_3$ gel exhibited a C-shaped (linear) isotherm and 21% of adsorbed ofloxacin was released from the mineral surface during desorption reactions [15]. Al dissolution and changes in solution pH as a function of ofloxacin adsorption were not measured in either study. Thus, it is unclear to what extent aqueous Al may compete with Al surfaces for ofloxacin complexation, and the multifunctionality of this compound may equate to several possible bonding mechanisms.

Nowara et al. [16] investigated the sorption of several FQCAs, including levofloxacin (an active optical isomer of ofloxacin), to soil, soil clay fractions, and soil minerals. This study reported that adsorption of FQCAs to soil, soil clay fractions, and layer silicates is very high (95–99% removal from initial aqueous concentrations ranging from 0.28 to 28 μmol L^{-1}) and desorption in 0.01 M $CaCl_2$ is very low (<2.6% of adsorbed amount was released into solution). Infrared spectra and microcalorimetry data were interpreted by Nowara et al. [16] to suggest that FQCAs are bound to clays via a cation bridge between charged basal surfaces and the carboxylate functional group of FQCAs [16]. However, cation bridging is a relatively weak sorption mechanism that is not associated typically with irreversible adsorption as observed by Norwara et al. [16]. In addition, experimental pH values were generally equal to or less than the pK_{a1} of the FQCAs, thus cationic forms of the compounds may have been adsorbed to mineral surfaces. High K_{oc} values (40,000–71,000) suggest that sorption was also influenced by the amount of organic carbon present in the soil [16], and others have reported sorption of FQCAs to dissolved humic acids [17,18].

An additional factor that should be considered when studying the fate of organic compounds in soils and sediments is substrate surface morphology. Recent studies have demonstrated that mineral mesoporosity (2–50 nm in pore diameter), as occurs in naturally weathered geosorbents [19], can impact organic compound sorption. Zimmerman et al. [20] observed that nitrogenous organic compounds smaller than one-half the average mesopore diameter exhibited significantly greater surface area-normalized adsorption to mesoporous alumina and silica, relative to nonporous analogues. Sorption of larger compounds was inhibited due to compound exclusion from the internal mesopore surfaces. Goyne et al. [21] documented increased adsorption of the pesticide 2,4-D to alumina sorbents with increased mesoporosity. However, it should be noted that porosity, in and of itself, is not always the most important governing factor. For instance, 2,4-D did not adsorb to mesoporous or nonporous silica, presumably because of electrostatic repulsion [21].

In this work, studies were conducted to investigate the sorption of the FQCA ofloxacin to nonporous and mesoporous Al_2O_3 and SiO_2 mineral sorbents. The objectives of this study were (a) to investigate differences in ofloxacin sorption to Al_2O_3 and SiO_2 surfaces as a function of pH and initial concentration, (b) to determine if mesoporosity influences the amount of ofloxacin sorbed to Al_2O_3 and SiO_2 solids, and (c) to determine the mechanism(s) through which ofloxacin binds to Al_2O_3 and SiO_2 surfaces.

2. Materials and methods

2.1. Properties of the adsorbate

Ofloxacin (9-fluoro-2,3-dihydro-3-methyl-10-(4-methyl-1-piperanzinyl)-7-oxo-7H-pyrido[1,2,3-*de*]-1,4-benzoxazine-6-carboxylic acid; 98% minimum purity) was purchased from Sigma–Aldrich Co. (St. Louis, MO) and used as received. The compound was stored at 4 °C in the dark to minimize photolytically induced degradation [22]. Ofloxacin is a zwitterionic compound with acid dissociation constants of 6.08 (pK_{a1}) and 8.25 (pK_{a2}) (Fig. 1) [12,23]. As shown in Fig. 1b, the antibiotic is primarily cationic below pK_{a1} (N_4 in the piperazinyl group), anionic above pK_{a2} (3-carboxyl

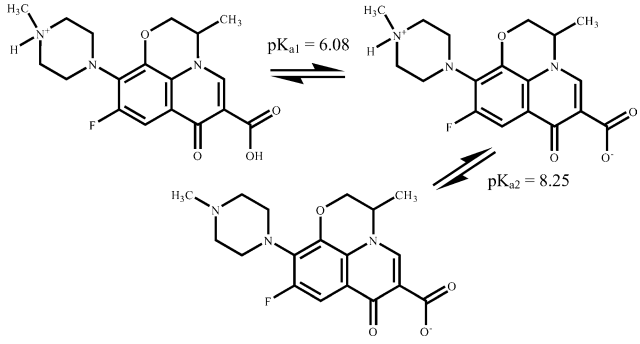

(a)

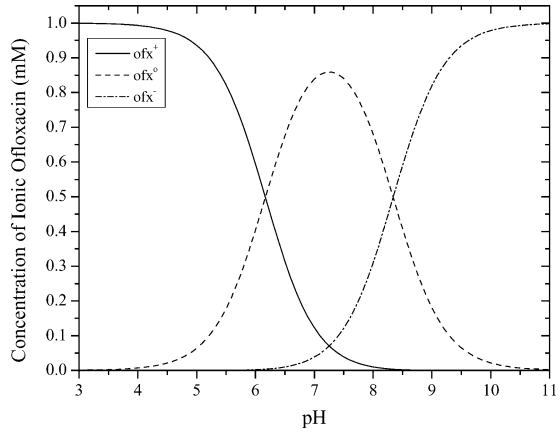

(b)

Fig. 1. (a) Ionization of aqueous ofloxacin and (b) distribution of cationic (ofx^+), zwitterionic (ofx^0), and anionic (ofx^-) ofloxacin in aqueous solution as a function of pH ($pK_{a1} = 6.08$ and $pK_{a2} = 8.25$) [10,21].

group), and zwitterionic (net neutral) between pK_{a1} and pK_{a2}. Due to solubility issues ($C_w^{sat} = 9$ mM at pH 7), ofloxacin stock solutions were not prepared at concentrations greater than 9 mM [23]. The dimensions of ofloxacin as determined by measuring interatomic distances and accounting for van der Waals radii of the atoms and constrained by energy minimization using the COMPASS force field are $1.2 \times 0.95 \times 0.6$ nm.

2.2. Adsorbent synthesis and characteristics

Four mineral adsorbents were used in the present work: (1) mesoporous Al_2O_3 (Al-P_{242}), (2) nonporous Al_2O_3(Al-NP_{37}), (3) mesoporous SiO_2 (Si-P_{700}), and (4) nonporous SiO_2 (Si-NP_8), where the subscripts refer to specific surface area in $m^2\,g^{-1}$. Al-NP_{37} and Si-NP_8 were purchased from Alfa Aesar (Ward Hill, MA), Stock Nos. 40007 and 89709, respectively. Al-NP_{37} was washed and dried as described in Goyne et al. [24] to remove an N-containing soluble constituent associated with synthesis. Adsorbents Al-P_{242} and Si-P_{700} were prepared using a neutral template route [25–27]. The synthesis procedure and removal of the templates from the fabricated adsorbents are detailed elsewhere [24,25]. All minerals, except Si-NP_8, were ground gently prior to characterization and stored in polyethylene bottles prior to use. The physical and chemical characteristics were published previously [24], and a summary is provided in Table 1.

2.3. Batch sorption edge and isotherm experiments

Mineral adsorbents were suspended in a 0.02 M $CaCl_2$ (0.06 M ionic strength) background electrolyte solution to give a sorbent surface area to solution ratio of $2.86 \times 10^3\,m^2\,L^{-1}$ in PTFE centrifuge tubes. Sorption experiments were conducted in the absence of pH buffers to prevent competitive sorption between buffer constituents (e.g., phosphate) and ofloxacin for available sorption sites and to allow for measurement of pH shifts often indicative of ligand exchange reactions [28]. All stock solutions or samples containing ofloxacin were wrapped in aluminum foil and/or stored in amber glassware to prevent or minimize photodegradation.

Solutions of 0.06 M HCl or 0.02 M $Ca(OH)_2$ were added to mineral suspensions (prior to reaction) to achieve a final pH range from pH 2 to 10 for sorption edge experiments and pH 7.2 for isotherm experiments. Samples were spiked with ofloxacin dissolved in 0.02 M $CaCl_2$ to give initial ofloxacin concentrations ranging from 0.03 to 8 mM for isotherm experiments or 1 mM for sorption edge experiments. Although these concentrations are significantly greater than those detected in natural waters [2,5–7], our goal was to compare ofloxacin sorption to mesoporous and nonporous silica and alumina, not to mimic solute concentrations found in impacted waters. For the isotherm experiments, the initial pH of the ofloxacin stock solution and $CaCl_2$ solution was adjusted to 7.20. Samples were reacted on an end-over-end shaker (7 rpm) in the dark at 298 K for 30 min. Adsorbent-free controls (no mineral) were reacted concurrently to measure compound loss resulting from sorption to centrifuge tube walls or volatilization. Neither of these was found to be significant.

After reaction, mineral suspensions were centrifuged at $15{,}290g$ and 298 K for 45 min. An aliquot of supernatant solution was removed by pipet, stored in 4 ml amber vials, and refrigerated for measurement of ofloxacin concentration. The remaining solution was aspirated, filtered through a 0.02-μm nominal pore size filter, acidified to pH < 2 with trace metal grade HCl, and refrigerated at 4 °C. Concentrations of Al and Si were determined using a Perkin–Elmer Elan DRC II inductively coupled plasma-mass spectrometer (ICP-MS). The pH of unfiltered and unacidified supernatant solution was measured using a calibrated Orion Ross semi-micro combination pH electrode attached to a Beckman Φ 390 pH meter.

Ofloxacin concentrations in solution were determined by measuring the concentration of nonpurgable organic carbon (NPOC) and total nitrogen (TN) present in solutions acidified to pH < 2 with trace metal grade HCl (Shimadzu Model TOC-V_{CSH}, total organic carbon analyzer, equipped with a TNM-1, total nitrogen measuring unit, and an ASI-V autosampler). Standards were prepared by dissolving ofloxacin in 0.02 M $CaCl_2$. There were no significant differences between ofloxacin concentrations calculated using NPOC or TN; thus all data shown are based on NPOC measurements for simplicity. High-performance liquid chromatography (HPLC) was not used, due to decreased column retention of ofloxacin when aluminum was present in solution (i.e., peaks were broadened and decreased in height,

Table 1
Physical characteristics and surface charge properties of the adsorbents

Adsorbent	S_{BET} ($m^2\,g^{-1}$)	D_{pore} (nm)	S_{ip} (%)	p.z.n.c.	pK_{a1}	pK_{a2}
Si-P_{700}	700 ± 10	3.4 ± 0.4	99.7	<2.85	NA	6.85 ± 0.63
Si-NP_8	7.5 ± 0.1	14 ± 2	NA	<2.82	NA	7.74 ± 0.27
Al-P_{242}	242 ± 6	8.2 ± 0.6	96.5	6.47 ± 0.05	6.19 ± 0.62	6.93 ± 0.78
Al-NP_{37}	37 ± 3	20 ± 3	NA	6.66 ± 0.06	6.58 ± 0.67	7.14 ± 0.83

Note. See Goyne et al. [21] for detailed methods and data analysis; S_{BET} is the specific surface area ± std. dev. as measured by N_2 BET; D_{pore} is the mean pore diameter ± std. dev. determined by the BJH method on the adsorption isotherm leg; S_{ip} is the intraparticle surface area (within pores 2–20 nm in diameter) as percentage of total determined by BJH method; p.z.n.c. is the point of zero net charge ± 95% CI; values of p.z.n.c. not encountered in the pH range of the experiment are expressed as the lowest pH values of the experiment; pK_{a1} and pK_{a2} are surface acidity intrinsic constants in accordance with the constant capacitance model, using proton charging data from [21].

evidently because of ofloxacin complexation with Al in the aqueous phase). However, excellent agreement between standards analyzed using HPLC and NPOC/TN was observed in the absence of aluminum. Mineral blanks (no ofloxacin) were reacted concurrently for correction.

Surface excess of ofloxacin was calculated as

$$\Gamma_{\text{ads}} = \frac{C_{\text{ads,B}} - C_{\text{ads,S}}}{SA_{\text{S}}}, \quad (1)$$

where Γ_{ads} is the surface excess of ofloxacin ($\mu\text{mol m}^{-2}$), $C_{\text{ads,S}}$ and $C_{\text{ads,B}}$ are the equilibrium ofloxacin concentrations ($\mu\text{mol kg}^{-1}$) in supernatant solutions of mineral suspensions (S) and for the corresponding blank (B) after the reaction period, and SA_{S} is the suspension concentration of adsorbent ($\text{m}^2\,\text{kg}^{-1}$).

Desorption reactions (isotherm experiments only) were initiated immediately after the adsorption step by adding a mass of 0.02 M $CaCl_2$ (pH 7.20) equivalent to that mass of supernatant solution removed. Desorption reaction time was equal to that for adsorption (30 min). After the desorption period, supernatant solutions were again removed by pipet and analyzed. Adsorbate retained was calculated from

$$\Gamma_{\text{des}} = \Gamma_{\text{ads}} - \left\{ \frac{(C_{\text{des,S}})(M_{\text{tot,soln}}) - (C_{\text{ads,S}})(M_{\text{ent}})}{SA} \right\}, \quad (2)$$

where Γ_{des} is the surface excess of ofloxacin ($\mu\text{mol m}^{-2}$) after the desorption step, $C_{\text{des,S}}$ is the ofloxacin concentration in supernatant solution of mineral suspension (S) after the desorption reaction ($\mu\text{mol kg}^{-1}$), $M_{\text{tot,soln}}$ is the total mass of solution (kg) in the reaction vessel during desorption, M_{ent} is the mass of entrained solution (kg) remaining in the centrifuged adsorbent pellet after aspiration of adsorption step supernatant, and SA is the total surface area of adsorbent (m^2) in the reaction vessel.

Sorption data were fit to the Langmuir–Freundlich equation [29] which has been shown to successfully model a number of other organic compounds on heterogeneous surfaces [20,30]:

$$q_i = \frac{N_{\text{t}} A c_i^{\beta}}{1 + A c_i^{\beta}}, \quad (3)$$

where q_i is adsorbate surface excess ($\mu\text{mol m}^{-2}$), N_{t} is the total number of binding sites, A is a parameter related to the binding affinity (K_0; $K_0 = A^{1/\beta}$), c_i is the equilibrium aqueous concentration of ofloxacin ($\mu\text{mol L}^{-1}$), and β is a fitting parameter [20,30,31]. When $\beta = 1$, the Langmuir–Freundlich equation reduces to the Langmuir equation

$$q_i = \frac{N_{\text{t}} A c_i}{1 + A c_i} \quad (\beta = 1), \quad (4)$$

whereas, if c_i or A approach zero, it equation reduces to the Freundlich equation

$$q_i = A c_i^{\beta} \quad (c_i \text{ or } A \to 0). \quad (5)$$

The Langmuir–Freundlich equation was fit to the experimental data using the method outlined in Umpleby et al. [29], where the solver function of Microsoft Excel 2002 is used to vary iteratively the three fitting parameters N_{t}, A, and β to maximize the coefficient of determination ($R^2 = 1$).

2.4. Infrared spectroscopy

Attenuated total reflectance (ATR)–Fourier transform infrared (FTIR) spectroscopy was employed to document changes in ofloxacin spectra as a function of pH and ionic composition and to investigate the mechanism of adsorption. For aqueous phase spectra, stock solutions containing 9.0 mM ofloxacin were prepared in 0.06 M NaCl and 0.02 M $CaCl_2$ background electrolyte solutions with pH values ranging from pH 5 to 10. A 3-ml aliquot of solution was then transferred into an ATR cell equipped with a 45° ZnSe flat plate crystal (ARK cell, Thermo Spectra-Tech, Inc.), and spectra were obtained by averaging 400 scans at 2 cm^{-1} resolution on a Nicolet Magna 560 spectrometer.

Infrared spectra of adsorbed ofloxacin were obtained for samples containing 11.80 g L^{-1} of mesoporous material reacted at pH 5.5 and 7.2 for 30 min with initial ofloxacin concentrations of 0 and 9.0 mM, as described previously. After adsorption, samples were centrifuged and most of the supernatant solution was removed, except ca. 3.0 ml which was left in the suspension to create a slurry. ATR–FTIR slurry samples were immediately transferred into the ATR cell for data collection. Spectra of adsorbed ofloxacin were obtained by subtracting those of the ofloxacin-free slurry.

2.5. Molecular modeling of infrared frequencies

Gas-phase, infrared frequencies of cationic, anionic, zwitterionic ofloxacin, and an Al–ofloxacin complex were calculated at the B3LYP/6-31G(d) level [32–34] using the Gaussian 98 program [35]. Frequency values were corrected by multiplying calculated values by 0.96 [36]. Model structures of the cationic, zwitterionic, and anionic species of ofloxacin were modeled with and without explicit hydration of the polar functional groups. In addition, the species $(OH_2)_4$Al–ofloxacin (in the zwitterionic state) was modeled. The Al^{3+} was bonded in a bidentate fashion to one O atom of the carboxylate group and to the O atom of the adjacent ketone group. The output files were then used to view animated vibrational motions in Molden Version 3.9 [37] for band assignment.

3. Results and discussion

3.1. Ofloxacin adsorption as a function of pH

The effects of pH on ofloxacin adsorption to SiO_2 surfaces are shown in Fig. 2a. Above pH 5.0, Si-P_{700} adsorbs significantly more ofloxacin than does Si-NP_8. Maximum ofloxacin sorption to these minerals (80.3 and 67.2% for

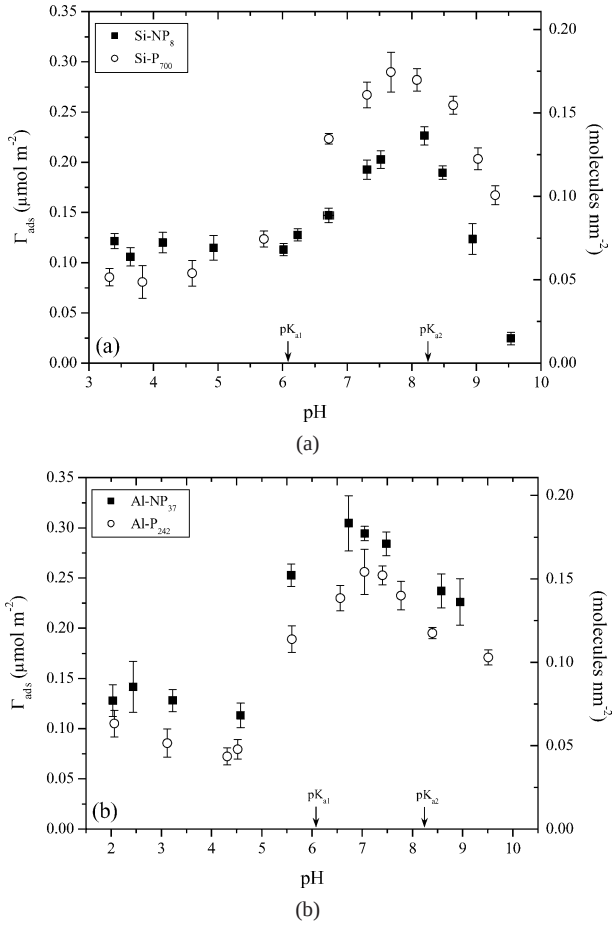

Fig. 2. Ofloxacin adsorbed (Γ_{ads}) on (a) Si-NP_8 and Si-P_{700} or (b) Al-NP_{37} and Al-P_{242} as a function of pH after 30 min of reaction time (duplicate means are shown and error bars, where visible, represent 95% CI). Surface excess is expressed as micromoles per square meter and molecules per square nanometer.

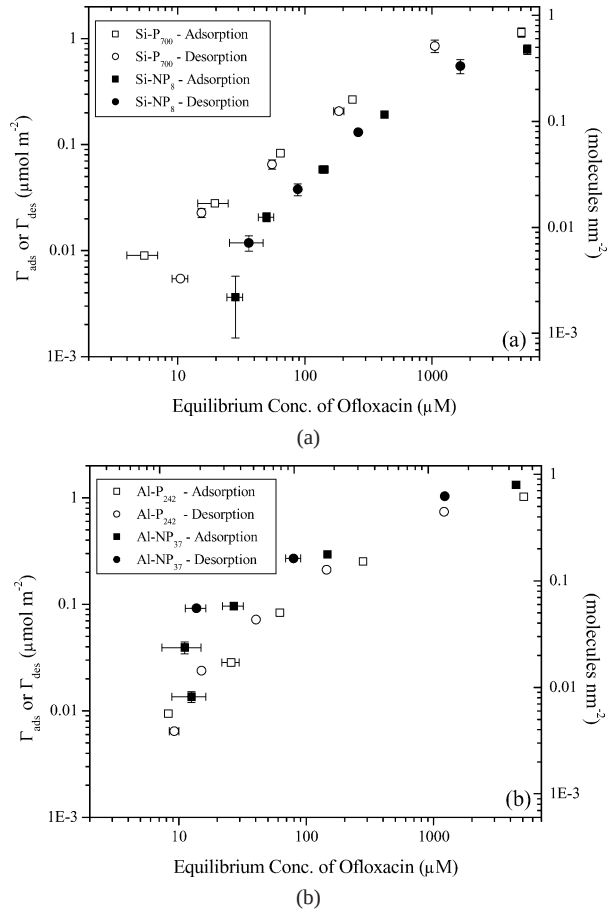

Fig. 3. Ofloxacin sorbed on (a) Si-NP_8 and Si-P_{700} or (b) Al-NP_{37} and Al-P_{242} after 30 min of adsorption (Γ_{ads}) or desorption (Γ_{des}) reaction time (duplicate means are shown and error bars, where visible, represent 95% CI). Surface excess is expressed as micromoles per square meter and molecules per square nanometer.

Si-P_{700} and Si-NP_8, respectively) occurs slightly below the pK_{a2} (pH 8.28) of the antibiotic and diminishes rapidly at pH > pK_{a2}. Thus, we presume that cationic and zwitterionic ofloxacin are adsorbed to the negatively charged silica surfaces (i.e., $\equiv SiO^-$ functional groups) via the protonated N_4 in the piperazinyl group. At the pH of maximum measured sorption, only 45 and 9% of the dissociated silanol groups on the surface of Si-P_{700} and Si-NP_8 [24], respectively, are occupied by the compound, suggesting that sorption was not limited by the availability of $\equiv SiO^-$ sites.

The fact that Si-NP_8 adsorbs more ofloxacin below pH 5 than does Si-P_{700} can be attributed to 50% higher density of dissociated surface silanol groups on Si-NP_8 at pH 3–5 according to surface charge data reported previously [24]. However, at this pH, Si-P_{700} has a greater fraction of dissociated silanol groups occupied by ofloxacin. For instance, ofloxacin sorbed onto Si-P_{700} at pH 3.32 occupies 62% of the $\equiv SiO^-$ groups, whereas at pH 3.40 ofloxacin occupies only 34% of the $\equiv SiO^-$ groups on Si-NP_8. Overall, it appears that the presence of intraparticle mesoporosity increases ofloxacin sorption to SiO_2 surfaces.

In contrast, Fig 2b indicates that ofloxacin sorption to mesoporous Al_2O_3 (Al-P_{242}) was consistently lower than sorption to nonporous Al_2O_3 (Al-NP_{37}) over the full pH range investigated. Sorption of the antibiotic to Al_2O_3 solids increases significantly above pH 5.0, concurrent with increased aqueous concentrations of zwitterionic ofloxacin. In this case, Γ_{max} (88.2 and 73.3% for Al-NP_{37} and Al-P_{242}, respectively) occurs at pH slightly less than midway between the pK_a values of ofloxacin (pH 7.16) and slightly higher than the adsorbent point of zero net charge (p.z.n.c.; Table 1). At pH greater than that of Γ_{max}, adsorption diminishes as alumina surfaces become increasingly negatively charged, thus repelling zwitterionic and anionic ofloxacin from the surface. These data lead us to hypothesize that ofloxacin sorption to $\equiv AlOH_2^+$ surface sites via the dissociated 3-carboxyl group (COO^-) of the zwitterion is initiated between pH 4.5 and 5.5. Initiation likely occurs closer to pH 5.5 based on Fig. 1b. However, the same mechanism of sorption may not be applicable below pH 5.0.

Ofloxacin adsorption to Al_2O_3 *decreases* from pH 2 to 4.5, and the same reproducible trend appears in the data sets for both alumina solids (Fig. 2b). We are unable to ex-

Table 2
Langmuir–Freundlich parameters for SiO_2 and Al_2O_3 isotherms

Adsorbent	Reaction phase	N_t (μmol m^{-2})	A (μM^{-1})	β	K_0 (μM^{-1})	R^2 (n)
Si-NP_8	Adsorption	0.80	4.6×10^{-5}	1.5	1.3×10^{-3}	0.96 (10)
	Desorption	0.63	5.7×10^{-5}	1.5	1.8×10^{-3}	0.96 (9)
Si-P_{700}	Adsorption	1.5	1.2×10^{-3}	0.94	8.2×10^{-4}	1.00 (9)
	Desorption	1.5	4.8×10^{-4}	1.1	1.1×10^{-3}	0.97 (9)
Al-NP_{37}	Adsorption	1.4	1.3×10^{-3}	1.1	2.3×10^{-3}	0.92 (10)
	Desorption	2.6	7.0×10^{-3}	0.65	4.5×10^{-4}	1.00 (6)
Al-P_{242}	Adsorption	1.2	9.5×10^{-4}	1.0	1.1×10^{-3}	1.00 (10)
	Desorption	0.78	5.6×10^{-4}	1.4	4.1×10^{-3}	0.98 (10)

Note. N_t is adsorption capacity; A is a parameter related to mean binding affinity (K_0); β is an exponent related to the heterogeneity of binding site energy distribution; K_0 is the mean binding affinity; R^2 is the coefficient of determination, and n is the number of sample points utilized to calculate the parameters.

plain the cause of this occurrence, other than to suggest that the mechanism of ofloxacin adsorption is likely different than above pH 5.0. Below pH 5, the fraction of zwitterionic ofloxacin is very low (Fig. 1b) and surface complexation via COO^- is likely insignificant. It is possible that dissolution of Al at acidic pH promotes the formation of Al-bridged dimers [36] whose adsorption could be enhanced relative to monomeric ofloxacin. Irrespective of the mechanism(s) of adsorption, it is clear that intraparticle porosity does not increase sorption of ofloxacin to alumina surfaces. This is despite the fact that ofloxacin is smaller ($1.2 \times 0.95 \times 0.6$ nm) than the nominal pore size of Al-P_{242} (8.2 nm) and that these alumina minerals have nearly identical surface charge properties [24].

3.2. Ofloxacin adsorption/desorption isotherms

Adsorption/desorption experiments were conducted to investigate ofloxacin sorption and retention as a function of initial sorptive concentration at a target equilibrium pH 7.20 (Fig. 3). The isotherm data agree with findings from sorption edge experiments in that mesoporous SiO_2 consistently sorbs more ofloxacin than nonporous SiO_2 (Fig. 3a); whereas, the opposite is true for Al_2O_3 adsorbents (Fig. 3b).

The Langmuir–Freundlich isotherm results in Table 2 indicate that N_t (sorption maximum) and A (measure of binding affinity) for the two minerals adsorbing greater amounts of ofloxacin are very similar and higher than the lower affinity sorbents. In addition, values of N_t indicate that whereas the sorption maximum was reached by Si-NP_8, adsorption to the other minerals is below the predicted maximum. No other discernible trends are apparent within the Langmuir–Freundlich isotherm parameters.

As mentioned under Section 2, isotherm experiments were conducted in the absence of pH buffers. Thus, ofloxacin stock solution and 0.02 M $CaCl_2$ background electrolyte solution were adjusted with base (0.02 M $Ca(OH)_2$) to pH 7.20, and additional acid (0.06 M HCl) or base was added at the beginning of each experiment to offset any pH changes resulting from buffering of the minerals themselves [24]. The amount of acid/base added to reaction vessels was constant for the full isotherm of each adsorbent to permit measurement of proton or hydroxide production, but varied among the four adsorbents.

Equilibrium pH values for SiO_2 samples were relatively constant (pH 7.20–7.40) except for those reacted at the highest initial concentration of ofloxacin (pH 6.77 and 6.65 for Si-NP_8 and Si-P_{700}, respectively). This proton production likely decreased the quantity of ofloxacin sorbed to these samples, relative to that adsorbed at pH 7.20 (see Fig. 2a), and may slightly skew the isotherm shapes shown in Fig. 3a. However, this shift to more acidic pH is indicative of proton displacement from ≡SiOH surface functional groups. This is verified by comparing the moles of ofloxacin adsorbed to the predicted density of $\equiv SiO^-$ present at equilibrium pH for samples with the highest initial ofloxacin concentration. At pH 6.78, 0.79 μmol m^{-2} of ofloxacin is adsorbed to Si-NP_8 and the predicted density of $\equiv SiO^-$ at this pH is 0.74 μmol m^{-2}. However, 1.15 μmol m^{-2} of ofloxacin is adsorbed to Si-P_{700} with a predicted dissociated silanol site density of 0.34 μmol m^{-2} at pH 6.65. Thus cationic ofloxacin is displacing adsorbed protons upon adsorption:

$$\equiv SiOH + ofx^+ \rightleftarrows \equiv SiO\text{–}ofx + H^+. \quad (6)$$

Calculations show that for Si-NP_8 the stoichiometry of this cation exchange reaction is 1:1 as shown in Eq. (6). For Si-P_{700}, the measured release of H^+ is somewhat lower than the moles of ofloxacin adsorbed in excess of negatively charged sites, suggesting the possibility of additional sorption mechanisms (e.g., cation bridging).

In contrast, pH values for Al_2O_3 reacted samples show an *increase* in pH with increased ofloxacin adsorption, regardless of whether acid or base was added to reach the target equilibrium pH of 7.20. The range of Al_2O_3 sample pH values (pH 6.45–7.58) are located very near maximum adsorption (see Fig. 2b), and the shape of the Al_2O_3 isotherms should be very similar to that of isotherms where pH = 7.20 for all samples. These results are suggestive of ligand exchange reactions between $\equiv AlOH_2^+$ and the COO^- of ofloxacin [26]:

$$\equiv AlOH + ofx^0 \rightleftarrows \equiv Al\text{–}ofx^+ + OH^-. \quad (7)$$

This could explain the slight hysteresis between the Al_2O_3 adsorption/desorption isotherms (Fig. 3b), and adsorption

via the COO^- functional group agrees with the sorption mechanism inferred from sorption edge experiments (Fig. 2b). Dissolution data for Al adsorbents are very similar and show elevated Al concentrations in solution (582 and 593 μM for Al-P_{242} and Al-NP_{37}, respectively) for samples reacted with the highest initial concentration of ofloxacin, relative to mineral controls (<6.4 μM) and solubility data published previously for these materials (<1.4 μM) [22]. This is also consistent with adsorption via a ligand exchange reaction, which would tend to promote Al dissolution [38].

3.3. Infrared spectra of dissolved ofloxacin and ofloxacin–adsorbent complexes

Although several studies have used infrared spectroscopy to investigate the interaction of ofloxacin with polyvalent cations [14,39–41], these studies have not documented changes in aqueous phase spectra as a function of pH (i.e., functional group protonation) and cation composition (i.e., aqueous phase complexation). Thus, as noted by Macias et al. [14], assigning functional groups appropriately to vibrations observed in powder IR spectra of ofloxacin–metal complexes can be challenging. In order to help interpret ATR–FTIR spectra of ofloxacin adsorbed to the mineral surfaces, we first collected ATR–FTIR difference spectra of ofloxacin (9 mM) dissolved in 0.06 M NaCl and 0.02 M $CaCl_2$ from pH 5 to 10 as shown in Figs. 5 and 6. (Difference spectra were obtained by subtracting spectra of the background electrolyte solutions at a particular pH from their counterparts containing dissolved ofloxacin.) Ofloxacin dissolved in the different background electrolyte solutions were compared because it is known that ofloxacin forms strong bonds with divalent cations [11,12,14,39–41], possibly through interaction between the carboxylic and ketone groups [40,41].

In Fig. 4, we observe that the C=O stretch of COOH (1710 cm^{-1}) [14,39–42] is lost as pH increases. Subsequently, intensity of the asymmetric (1585 cm^{-1}) [42] and symmetric (1340 cm^{-1}) [42] stretch of COO^- increases with increasing pH. There is also an increase in the intensity of the wavenumber that we assign as vibrations associated with protonation of N_4 in the piperazinyl group (1400 cm^{-1}) [43]. Assignments of the remaining vibrations observed in Fig. 4 are as follows: C=O stretch of ketone group (1620 cm^{-1}) [14,39,40], C=C aromatic stretching (1530 cm^{-1}) [42], and C–O–C stretching of the ether group (1055 cm^{-1}) [14,39,42].

Molecular orbital models of ofloxacin calculations on the explicitly solvated models generally produce similar frequencies (±35 cm^{-1}; Table 3) for the main peaks of interest. The C=O stretch of the carboxylic acid for explicitly solvated cationic ofloxacin is an exception because it is calculated to occur at 80 cm^{-1} lower than the experimental observation. The main reason for this discrepancy is the approximate representation of the electron correlation in the

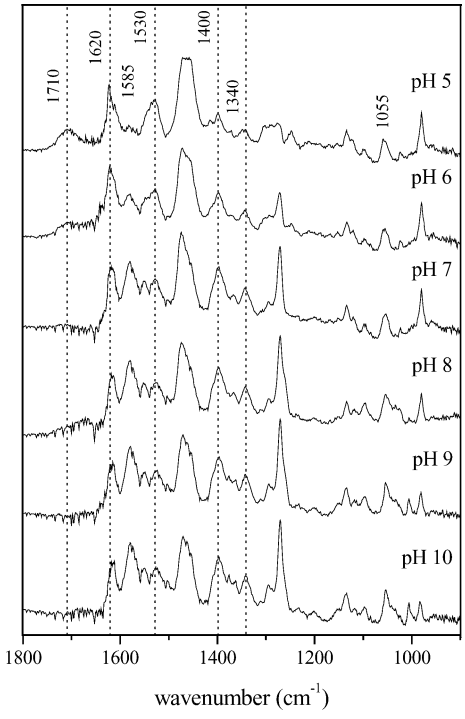

Fig. 4. Attenuated total reflectance–Fourier transform infrared (ATR–FTIR) difference spectra of ofloxacin in 0.06 M NaCl from pH 5 to 10. Difference spectra were obtained by subtracting spectrum of 0.06 M NaCl at a particular pH from spectrum of ofloxacin dissolved in 0.06 M NaCl at the same pH.

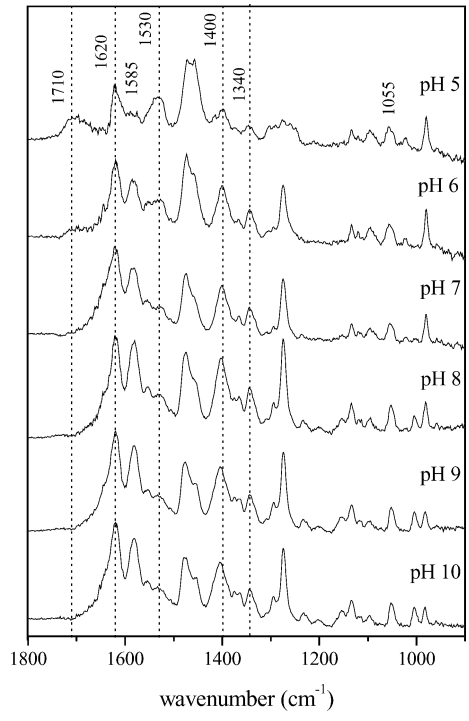

Fig. 5. Attenuated total reflectance–Fourier transform infrared (ATR–FTIR) difference spectra of ofloxacin in 0.02 M $CaCl_2$ from pH 5 to 10. Difference spectra were obtained by subtracting spectrum of 0.02 M $CaCl_2$ at a particular pH from spectrum of ofloxacin dissolved in 0.02 M $CaCl_2$ at the same pH.

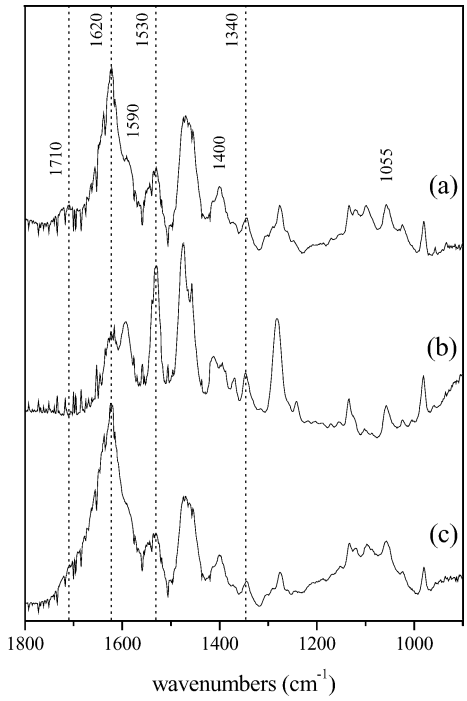

Fig. 6. Attenuated total reflectance–Fourier transform infrared (ATR–FTIR) difference spectra of (a) ofloxacin in 0.02 M $CaCl_2$ at pH 5.5 and ofloxacin-adsorbent slurry at pH 5.5 for (b) Al-P_{242} and (c) Si-P_{700}. Difference spectra were obtained by subtracting spectrum of 0.02 M $CaCl_2$ from ofloxacin dissolved in 0.02 M $CaCl_2$ (a) and by subtracting 0.02 M $CaCl_2$-adsorbent slurry from ofloxacin–0.02 M $CaCl_2$-adsorbent slurry (b and c).

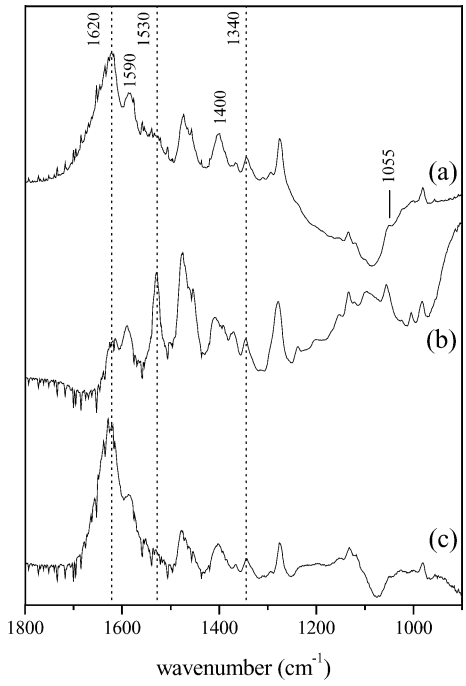

Fig. 7. Attenuated total reflectance–Fourier transform infrared (ATR–FTIR) difference spectra of (a) ofloxacin in 0.02 M $CaCl_2$ at pH 7.2 and ofloxacin-adsorbent slurry at pH 7.2 for (b) Al-P_{242} and (c) Si-P_{700}. Difference spectra were obtained by subtracting spectrum of 0.02 M $CaCl_2$ from ofloxacin dissolved in 0.02 M $CaCl_2$ (a) and by subtracting 0.02 M $CaCl_2$-adsorbent slurry from ofloxacin–0.02 M $CaCl_2$-adsorbent slurry (b and c).

molecule. Although the LYP gradient-corrected correlation functional is adequate for most of the bonds in the molecule, C=O bonds depend more strongly on electron correlation [44], so this calculated mode ends up with a larger discrepancy with experiment. A more accurate method for electron correlation could possibly decrease this error, but methods such as (MP2, Møller Plesset second-order perturbation) [45] require far more computational time and are not practical for a model of this size. However, without explicit solvation, COO^- stretching was predicted to occur in the 1725–1710 cm^{-1} region, an error of 100 cm^{-1} or more. In addition, linear regression of calculated versus predominant experimental frequencies ($n \geqslant 16$) for the three explicitly solvated molecules yielded slopes of 1 (± 0.03) and R^2 values of 0.99. Based on this good correlation, we conclude that the model calculations produce realistic vibrational frequencies for ofloxacin and can be used to help interpret spectra of unknown structures such as surface complexes.

Ofloxacin spectra collected in 0.02 M $CaCl_2$ (Fig. 5) show trends similar to those in Fig. 4 as pH increases, but vibrations associated with the ketone and asymmetric stretch of COO^- are more intense and broadened in the presence of Ca^{2+}. We propose, as have others [40], that this is indicative of a weak Ca–ofloxacin complex that forms between the ketone and carboxylate functional groups. Apparently, similar complexes are not formed in the presence of monovalent ions with a large hydrated radius (e.g., Na^+; Fig. 4).

Difference spectra of ofloxacin and ofloxacin–mineral complexes formed at pH 5.5 and 7.2 are shown in Figs. 6 and 7, respectively. (Difference spectra were obtained by subtracting a spectrum of mineral suspended in 0.02 M $CaCl_2$ at a specific pH from corresponding samples reacted with ofloxacin.) The spectra indicate that sorption of ofloxacin occurs via similar mechanisms for a given mineral type, irrespective of pH. For example, ofloxacin sorbed to Al_2O_3 at pH 5.5 (Fig. 6b) and 7.2 (Fig. 7b) shows a dramatic decrease in the intensity of the ketone (1620 cm^{-1}) and asymmetric COO^- (1590 cm^{-1}) vibrations. However, the same spectra show a large increase in the intensity of peaks at 1530 and 1275 cm^{-1}.

We attribute the change at 1530 cm^{-1} to a downward shift in frequency of the ketone and/or asymmetric COO^- stretch upon innersphere complexation with an Al center on the mineral surface. Molecular modeling of an ofloxacin–Al complex, whereby Al is bound via bidentate complexation to the ketone and carboxylate functional groups (Fig. 8) [10,13], indicates that the downward shift is attributable to the ketone vibration (predicted at 1525 cm^{-1}; Table 4). Although others have suggested that the ketone group vibration may decrease in frequency upon strong complexation with a metal ion [14,39], our experimental data and calculations demonstrate this occurrence, as do calculations performed by Sagdinc and Bayarı [41]. Perhaps more importantly, the

Table 3
Selected experimental and calculated vibrational frequencies for ofloxacin

Vibration	Experimental (cm^{-1})	Calculated (cm^{-1})
	pH 5	Cationic
C=O stretch of carboxylic acid	1705	1614, 1598
C=O stretch of ketone group	1622	1646
COO^- asymmetric stretching	1582	N.C.V.
C=C stretching	1530	1541
COO^- symmetric stretching	1344	N.C.V.
C–O–C stretching of ether group	1058	1075
	pH 7	Zwitterionic
C=O stretch of ketone group	1620	1646
COO^- asymmetric stretching	1579	1614
C=C stretching	1528	1541
COO^- symmetric stretching	1343	1336
C–O–C stretching of ether group	1054	1065
	pH 10	Anionic
C=O stretch of ketone group	1615	1644
COO^- asymmetric stretching	1579	1603
C=C stretching	1527	1533
COO^- symmetric stretching	1342	1342, 1348
C–O–C stretching of ether group	1053	1079

Note. Experimental assignments are reported for ofloxacin in 0.06 M NaCl; N.C.V. is no calculated vibration. However, the calculated results where N.V.C. is reported are reasonable. This is due to the presence of COOH, only, in the modeled cationic molecule; whereas, the experimental data contain both cationic (dominant) and zwitterionic (minor) species in solution.

IR data strongly support our hypothesis that ofloxacin sorbs to Al_2O_3 surfaces via a ligand exchange process [46–48].

In contrast, IR spectra of ofloxacin sorbed to SiO_2 (Figs. 6c and 7c) are similar to those of dissolved ofloxacin, despite the fact that Si-P_{700} adsorbed 2–3 times more ofloxacin per unit mass than did Al-P_{242} (Figs. 6b and 7b). However, the spectra of the ofloxacin–SiO_2 complex collected at pH 5.5 shows an increase and broadening of the

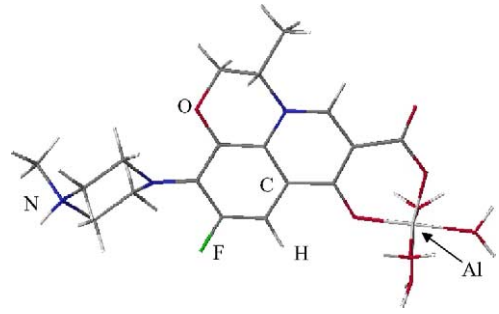

Fig. 8. Molecular structure of $(OH_2)_4$Al–ofloxacin (zwitterionic) complex. This complex has the same basic orientation as the ofloxacin molecules shown in Fig. 1a.

ketone frequency (1620 cm^{-1}). This suggests that ofloxacin may be bonded to SiO_2 surfaces via a cation bridge at pH 5.5, although the same occurrence is not observed at pH 7.2 (Fig. 7c). This supports our contention that ofloxacin sorbs to SiO_2 through the protonated piperazinyl group, via weaker electrostatic interaction, and through a cation bridge.

3.4. Mechanisms for enhanced or reduced ofloxacin sorption to mesoporous adsorbents

Enhanced ofloxacin sorption to mesoporous SiO_2 is hypothesized to occur due to higher concentration of Ca^{2+} ($[Ca^{2+}]$) within the confines of a pore. Our calculations indicate that electric double layer (EDL) thickness extending from a planar solid–water interface in 0.02 M $CaCl_2$ is 1.2 nm [49]. Given that the mean pore diameter of Si-P_{700} is 3.4 nm, EDLs within pore confines would not quite overlap near the center of this circular pore. However, the presence of EDLs extending from pore walls into the pore center should increase $[Ca^{2+}]$ and decrease $[Cl^-]$ in the pore, relative to concentrations of these ions near surfaces exter-

Table 4
Correlation of calculated vibrations and assignments of an Al–ofloxacin complex to experimental vibrations

Vibration	Calculated (cm^{-1})	Experimental (cm^{-1})
	Zwitterionic	
C=O stretch of carboxylate–Al complex	1755 (s)	1621
C=C stretching	1593 (m), 1572 (m)	1591
C=O stretch of ketone group	1525 (w)	1532
CH wag	1488 (s), 1468 (m)	1500–1450
C–O(C) stretch	1415 (m), 1413 (s)	1408
CH wag	1378 (m), 1372 (m)	1371
CH wag	1325 (m), 1322 (m)	1346
CH wag	1290 (w)	1278
CH wag	1257 (w)	1240
CH wag	1227 (m)	1226
Al–O–C(O)	1197 (m)	1200
CH wag	1174 (m)	1151
CH wag	1135 (w)	1134
C–H bend	1106 (w), 1075 (m)	1098
C–O–C stretch of ether group	1076 (m)	1055
C–H wag	959 (w)	1005
C–H wag	936 (w)	983

Note. Vibration assignments are based on model results and experimental vibrations are reported for ofloxacin–Al-P_{242} slurry spectra collected at pH 7.2 (Fig. 7b).

nal to pores [50]. The higher [Ca^{2+}] within pores would promote ofloxacin–Ca^{2+} complexation via the carboxylate group (Fig. 5) and effectively increase the amount of positive charge on an ofloxacin ion. Therefore, a zwitterionic ofloxacin molecule could bind to the surface via the protonated N_4 of the piperazinyl group and, at the same time, bind via a cation bridge as others have observed [16]. This appears to be a reasonable explanation for increased ofloxacin sorption to mesoporous Si-P_{700} and it agrees with our other data that suggest ofloxacin binds to Si-P_{700} surfaces by more than one mechanism.

It is unclear why adsorption to Al-NP_{37} exceeds that of Al-P_{242}. Ofloxacin sorption to Al-P_{242} is not reduced due to exclusion of the antibiotic from the pores, differences in surface charge properties, or increased dissolution of Al-P_{242} resulting in aqueous and solid phase Al competition for ofloxacin. In addition, ATR–FTIR and molecular orbital calculations indicate that ofloxacin forms a strong innersphere complex with surface aluminum molecules. Thus, we conclude that the coexistence of positive- and negative-charged sites on Al_2O_3 [24] may inhibit sorption of ofloxacin within the pore confines, relative to external surfaces. If ofloxacin sorbs to Al centers via the ketone and carboxylate groups, then over a wide range of pH the protonated N_4 of the piperazinyl group will be positioned toward the pore center. This may, depending on the local surface charge properties, result in an energy barrier that prohibits or hinders ofloxacin sorption to particular aluminol sites. In other words, repulsive forces between the protonated N_4 of the piperanzinyl groups and $\equiv AlOH_2^+$ surface functional groups may inhibit ofloxacin sorption within pore confines.

4. Conclusions

Intraparticle mesoporosity in SiO_2 solids was found to result in increased uptake of ofloxacin when adsorption was normalized to sorbent surface area. Relative to the nonporous solid, the presence of intraparticle porosity resulted in a statistically significant sorption enhancement throughout the isotherms and over most of the sorption edge for the porous silica adsorbent (Si-P_{700}). Observations of proton release in association with ofloxacin sorption and sorption in excess of the surface site density of $\equiv SiO^-$ groups (measured in absence of ofloxacin) indicate that the compound is capable of displacing protons complexed with silanol groups as it sorbs to SiO_2 surfaces via the protonated N_4 of the piperazinyl group. Conversely, ofloxacin adsorption to nonporous Al_2O_3 was significantly higher than that to mesoporous Al_2O_3 in both sorption edge and isotherm experiments. The observed hydroxyl release concurrent with ofloxacin adsorption and shifts in the frequency of ketone and increased intensity of carboxylate stretching vibrations are indicative of ligand exchange between ofloxacin and $\equiv AlOH$ or $\equiv AlOH_2^+$ surface sites. Decreased adsorption on porous Al_2O_3 is postulated to result from electrostatic repulsion from specific, but as yet undetermined, aluminol sites within pore cavities. Overall, the data indicate that intraparticle mesopores can enhance ofloxacin sorption to adsorbent minerals, but the degree of enhancement may be diminished or even reversed by other mitigating factors (e.g., surface charge properties).

Acknowledgments

The authors thank Mary Kay Amistadi for laboratory assistance, Sridhar Komarneni, Bharat Newalkar, and Stephen Stout for mineral synthesis and preparation, and Chad Trout for assistance with molecular modeling. Financial support was provided by the Penn State Biogeochemical Research Initiative for Education (BRIE) sponsored by NSF (IGERT) Grant DGE-9972759 and by the Penn State Materials Research Science and Engineering Center (MRSEC) sponsored by NSF Grant DMR-0080019. Andrew Zimmerman acknowledges donors to the American Chemical Society Petroleum Research Fund for partial support of this research, and James Kubicki acknowledges the support of Stony Brook-BNL collaboration to establish a Center for Environmental Molecular Sciences (CEMS). Computation was supported, in part, by the Materials Simulation Center, a Penn State MRSEC and MRI facility.

References

[1] A.K. Sharma, R. Khosla, A.K. Keland, V.L. Mehta, Indian J. Pharm. 26 (1994) 249.
[2] E.M. Golet, A.C. Alder, W. Giger, Environ. Sci. Technol. 36 (2002) 3645.
[3] C.G. Daughton, T.A. Ternes, Environ. Health Perspect. 107 (1999) 907.
[4] J. Tolls, Environ. Sci. Technol. 35 (2001) 3397.
[5] D.W. Kolpin, E.T. Furlong, M.T. Meyer, E.M. Thurman, S.D. Zaugg, L.B. Barber, H.T. Buxton, Environ. Sci. Technol. 36 (2002) 1202.
[6] A. Hartmann, E.M. Golet, S. Gartiser, A.C. Alder, T. Koller, R.M. Widmer, Arch. Environ. Contam. Toxicol. 36 (1999) 115.
[7] E.R. Campagnolo, K.R. Johnson, A. Karpati, C.S. Rubin, D.W. Koplin, M.T. Meyer, J.E. Eseeban, R.W. Currier, K. Smith, K.M. Thu, M. McGeehin, Sci. Total Environ. 299 (2002) 89.
[8] S.E. Jørgensen, B. Halling-Sørensen, Chemosphere 40 (2000) 691.
[9] P.T. Djurdjevic, M. Jelikic-Stankov, J. Pharm. Biomed. Anal. 19 (1999) 501.
[10] M. Sakai, A. Hara, S. Anjo, M. Nakamura, J. Pharm. Biomed. Anal. 18 (1999) 1057.
[11] D.L. Ross, C.M. Riley, Int. J. Pharm. 93 (1993) 121.
[12] H.-R. Park, K.-Y. Chung, H.-C. Lee, J.-K. Lee, K.-M. Bark, Bull. Korean Chem. Soc. 21 (2000) 849.
[13] P.T. Djurdjevic, M. Jelikic-Stankov, I. Lazarevic, Bull. Chem. Soc. Jpn. 74 (2001) 1261.
[14] B. Macías, M.V. Villa, I. Rubio, A. Castiñeiras, J. Borrás, J. Inorg. Biochem. 84 (2001) 163.
[15] M. Tanaka, T. Kurata, C. Fujisawa, Y. Ohshima, H. Aoki, O. Okazaki, H. Hakusui, Antimicrob. Agents Chemother. 37 (1993) 2173.
[16] A. Nowara, J. Burhenne, M. Spiteller, J. Agric. Food Chem. 45 (1997) 1459.
[17] H.-C.H. Lützhøft, W.H.J. Vaes, A.P. Freidig, B. Halling-Sørensen, J.L.M. Hermens, Environ. Sci. Technol. 34 (2000) 4989.

[18] Ph. Schmitt-Kopplin, J. Burhenne, D. Freitag, M. Spiteller, A. Kettrup, J. Chromatogr. A 837 (1999) 253.
[19] L.M. Mayer, Chem. Geol. 114 (1994) 347.
[20] A.R. Zimmerman, K.W. Goyne, J. Chorover, S. Komarneni, S.L. Brantely, Org. Geochem. 35 (2004) 355.
[21] K.W. Goyne, J. Chorover, A.R. Zimmerman, S. Komarneni, S.L. Brantley, J. Colloid Interface Sci. 272 (2004) 10.
[22] E. Fasani, A. Profumo, A. Albini, Photochem. Photobiol. 68 (1998) 666.
[23] D.L. Ross, C.M. Riley, Int. J. Pharm. 63 (1990) 237.
[24] K.W. Goyne, A.R. Zimmerman, B.L. Newalkar, S. Komarneni, S.L. Brantley, J. Chorover, J. Porous Mater. 9 (2002) 243.
[25] S. Komarneni, R. Pidugu, V.C. Menon, J. Porous Mater. 3 (1996) 99.
[26] P.T. Tanev, T.J. Pinnavaia, Science 267 (1995) 865.
[27] W. Zhang, T.R. Pauly, T.J. Pinnavaia, Chem. Mater. 9 (1997) 2491.
[28] W. Stumm, Chemistry of the Solid–Water Interface, Wiley, New York, 1992.
[29] R.J. Umpleby, S.C. Baxter, Y. Chen, R.N. Shah, K.D. Shimizu, Anal. Chem. 73 (2001) 4584.
[30] J.-Y. Yoon, H.-Y. Park, J.-H. Kim, W.-S. Kim, J. Colloid Interface Sci. 177 (1996) 613.
[31] J.-Y. Yoon, J.-H. Kim, W.-S. Kim, Colloids Surf. A 153 (1999) 413.
[32] A.D. Becke, J. Chem. Phys. 98 (1993) 5648.
[33] C.T. Lee, W.T. Yang, R.G. Parr, Phys. Rev. B 37 (1988) 785.
[34] W.J. Hehre, R. Ditchfield, J.A. Pople, J. Chem. Phys. 56 (1972) 2257.
[35] M.J. Frisch, G.W. Trucks, H.B. Schlegel, G.E. Scuseria, M.A. Robb, J.R. Cheeseman, V.G. Zakrzewski, J.A. Montgomery Jr., R.E. Stratmann, J.C. Burant, S. Dapprich, J.M. Millam, A.D. Daniels, K.N. Kudin, M.C. Strain, O. Farkas, J. Tomasi, V. Barone, M. Cossi, R. Cammi, B. Mennucci, C. Pomelli, C. Adamo, S. Clifford, J. Ochterski, G.A. Petersson, P.Y. Ayala, Q. Cui, K. Morokuma, D.K. Malick, A.D. Rabuck, K. Raghavachari, J.B. Foresman, J. Cioslowski, J.V. Ortiz, B.B. Stefanov, G. Liu, A. Liashenko, P. Piskorz, I. Komaromi, R. Gomperts, R.L. Martin, D.J. Fox, T. Keith, M.A. Al-Laham, C.Y. Peng, A. Nanayakkara, C. Gonzalez, M. Challacombe, P.M.W. Gill, B. Johnson, W. Chen, M.W. Wong, J.L. Andres, C. Gonzalez, M. Head-Gordon, E.S. Replogle, J.A. Pople, Gaussian 98 (Revision A.10), Gaussian, Pittsburgh, PA, 2001.
[36] M.W. Wong, Chem. Phys. Lett. 256 (1996) 391.
[37] G. Schaftenaar, J.H. Noordik, J. Comput. Aided Mol. Design 14 (2000) 123.
[38] G. Sposito, The Chemistry of Soils, Oxford Univ. Press, New York, 1989.
[39] B. Macías, M.V. Villa, M. Sastre, A. Castiñeiras, J. Borras, J. Pharm. Sci. 91 (2002) 2416.
[40] B.M. Sánchez, M.M. Cabarga, A.S. Navarro, A.D.G. Hurlé, Int. J. Pharm. 106 (1994) 229.
[41] S. Sagdinc, S. Bayari, J. Mol. Struct. 691 (2004) 107.
[42] R.M. Silverstein, G.C. Bassler, T.C. Morrill, Spectrometric Identification of Organic Compounds, fifth ed., Wiley, New York, 1991.
[43] A.L. Mattioda, D.M. Hudgins, C.W. Bauschlicher Jr., M. Rosi, L.J. Allamandola, J. Phys. Chem. A 107 (2003) 1486.
[44] J. Gauss, J. Chem. Phys. 99 (1993) 3629.
[45] C. Møller, M.S. Plesset, Phys. Rev. 46 (1934) 618.
[46] B. Gu, J. Schmitt, Z. Chen, L. Liang, J.F. McCarthy, Geochim. Cosmochim. Acta 59 (1995) 219.
[47] J. Chorover, M.K. Amistadi, Geochim. Cosmochim. Acta 65 (2001) 95.
[48] K. Vermöhlen, H. Lewandowski, H.-D. Narres, E. Koglin, Colloids Surf. A 170 (2000) 181.
[49] D.L. Sparks, Environmental Soil Chemistry, Academic Press, San Diego, 1995.
[50] Y. Wang, C. Bryan, H. Xu, P. Pohl, Y. Yang, C.J. Brinker, J. Colloid Interface Sci. 254 (2002) 23.